Effects of a Kind of Surface Groove on Flow Loss in Both Rectangular and Circular Ducts at Different Reynolds Numbers

MA Rong, MA Hongwei, ZHANG Zhenyang, ZHANG Jinghui

National Key Laboratory of Science and Technology on Aero-Engines, Collaborative Innovation Center of Advanced Aero-Engine, School of Energy & Power Engineering, Beihang University, Beijing, 100191, China

Pipes are widely used to transport gas, oil and water in industries. Drag reduction in pipes is an increasingly concerned problem to save energy. Some researches have indicated that the non-smooth surface with special structures can reduce flow loss. In this paper, an experimental investigation has been performed on the effects of a kind of surface groove on the drag in both rectangular and circular duct at different Reynolds numbers. In the experiment of the rectangular duct, total pressure at both inlet and outlet were measured. Static pressure on the wall was measured on the surface with smooth and grooved film respectively. In the circular duct, a boundary layer pressure probe was used to measure the total pressure distribution at both inlet and outlet. Four taps at inlet and outlet were used to measure static pressure. The loss coefficient is used to evaluate the effects of the surface groove on drag reduction. The experiment was conducted with the Reynolds number range from 1.28×10^4 to 2.57×10^4. The result shows a maximum drag loss reduction of approximately 2.4% in rectangular duct at Reynolds number of 2.4×10^4. A 10% reduction of pipe pressure loss by grooved surface is measured in circular duct at a Reynolds number of 3.0×10^5.

Keywords: drag reduction, surface groove, rectangular duct, circular duct

Introduction

Drag reduction in pipeline transportation has become an advanced research hot spot throughout the industry. Surface groove is a kind of method to reduce flow loss. Therefore, studying and developing a kind of surface groove for loss reduction and energy saving is concerned by researchers in recent years.

Grooved surfaces were originally developed at NASA Langley Research Center in the late 1970's. It was aimed to reduce the aerodynamic turbulent skin friction. Based on the study of NASA Langley(Walsh[1]), many streamwise microgrooved surface were tested to verify the effect of drag reduction. The results showed a 7-8% drag reduction caused by sharply peaked, symmetric V-groove riblets. However, the practical application of V-groove is terminated because it is easily worn off.

Gong Wu-Qi[6] investigated the mechanism of drag reduction by using riblets and found that the grooved structure could change the features of boundary layer. The averaged turbulent dynamic energy decreases by drag reduction of riblets.

In addition to the study in external flows, investigation to the effects of grooved surfaces on internal flows is fewer. Bushnell[7] has mentioned that the effects of riblets on internal flows may be different from that on external

Nomenclature

d	Diameter of circular duct (mm)	P_{ot}	Outlet total pressure (Pa)
D	Characteristic scale of model (mm)	P_{it}	Inlet total pressure (Pa)
H	Height of rectangular duct (mm)	Re	Reynolds number

h	Riblet height (mm)	U	Outlet flow velocity (m/s)
h^+	Non-dimensional riblet height (mm)	ρ	Air density
s^+	Non-dimensional riblet width (mm)	μ	Dynamic viscosity coefficient
$P_{1\text{-}8}$	Static pressure probe of rectangular duct	λ_{smo}	Loss coefficient of smooth surface
P_{os}	Outlet static pressure (Pa)	λ_{gro}	Loss coefficient of grooved surface

flows due to the mass flow constraint. J.J. Rohr[8] has discovered that the drag reducing performance of riblets is found to be similar in a wide variety of internal and external flows. More researches about effects of grooved structures on internal flows are needed to be carried out.

A.R. Moore and M.V. Lowson[9] have studied the drag reduction in a rectangular duct using riblets. It has been found that a maximum drag reduction of 10% occurs in fully developed turbulent flow. This figure is larger than the 6-8% drag reduction in external flow. It was also found that riblets delayed transition by 2−4% and caused some extension in the length of the transition process.

Ma Hongwei[10]has carried out an experimental study of the turbulent boundary layers on both groove and smooth surfaces. The measurement results indicate that the grooves can effectively reduce accumulation of low-speed fluids and directly affect the flow structures in the sublayer of the boundary layer and then modulate the flow field up to the buffer region and the logarithmic region by restraining development and interaction of the vortices. However, the drag reduction of this groove structure applied to pipe flow is still short of validation.

In this paper, based on the previous results, research is focused on the effects of surface groove on the drag reduction of rectangular duct and circular duct. In the experiment, a pipe test rig was set up, which was equipped with high-accuracy and high spatial-resolution flow measuring system, including boundary-layer pressure probe, traverse mechanism, pressure transducers, data-acquisition hardware and software. In the rectangular duct, total pressure was measured at both inlet and outlet. Static pressure on the wall was measured on the surface with smooth and grooved film respectively. Loss coefficient and loss reduction efficiency were employed to analyze the results of the experiment.

In the experiment of circular duct, pipe models with smooth and groove surfaces were designed and manufactured respectively. Total pressure was measured at both inlet and outlet. One boundary layer pressure probe was used to measure the total pressure distribution. This probe scanned the outlet attached to a traverse mechanism. Four taps at inlet and outlet were used to measure static pressure.

Experimental Facility and Test Technique

Rectangular duct

The air flow with a speed range from 7 to 12m/s was provided by an axial flow fan with a power of 65W, a rotating speed of 2870 r/min and a mass flow of 0.08−0.13 kg/s. The range of Reynolds number in experiment is from 1.28×10^4 to 2.57×10^4. A schematic diagram of the test rig is shown in Fig. 1.

The air flow entered the inlet duct then flowed through the contraction section. The shrink angle of the contraction section was 4.6°. The flow was fully developed at cross section A1 after straightening gratings. The working section was attached to the straightening section. The size of working section were 30mm ×200mm with a length of 1300mm. The environment temperature was 27℃.

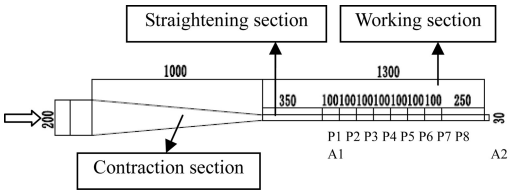

Fig. 1 Test rig of rectangular duct(mm)

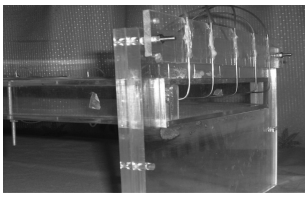

Fig. 2 Total pressure probes at outlet

On the surface of the working section, there were eight static pressure holes (with a diameter of 0.5mm) at 100mm intervals between every two holes which were used for the installation of eight static pressure probes. On cross section A2, five total pressure probes were configured at five different positions, shown in Fig. 2.

The measuring range of pressure sensor was from−1000Pa to +1000Pa with an error of 0.01%. An AT-MIO-64F-5 card from American NI Company was employed

for data acquisition. The frequency of data acquisition was 20K Hz. The experimental process was controlled by Labview.

Circular duct

The circular duct, shown in Fig.3, was attached to the contraction section of a windtunnel, which was driven by a roots blower.

The size of the duct model was 600mm long with an inner diameter of 115mm. The air flow was provided by the windtunnel with three different speeds of 10 m/s, 20 m/s and 30 m/s. The environment temperature was 27℃.

Total pressure was measured by one total pressure probe at inlet. In Fig. 4, one boundary layer pressure probe was used to measure the total pressure distribution at outlet. When it was near the inner wall, the station distance was 0.2 mm.When it reached the mainstream area, the station distance was 1 mm or 2 mm. The accuracy of the traverse mechanism was 0.02 mm. At inlet and outlet, there were four taps (with a diameter of 0.5 mm) used for static pressure measurement respectively. The static and total pressure taps were connected to the pressure transducers.

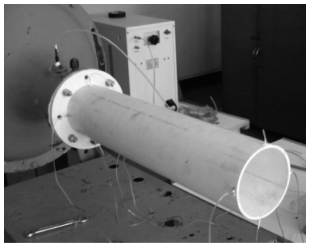

Fig. 3 Test rig of circular duct

Fig. 4 Boundary layer pressure probe

Groove structure

This paper studied the effect of one kind of groove structure on flow loss in a pipe. Fig.5 shows the geometry of the groove structure.

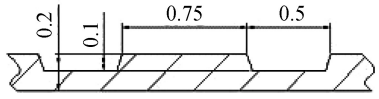

Fig. 5 Cross section of the test groove film (mm)

The non-dimensional riblet height h^+ is 2.24, while the non-dimensional riblet width s^+ is 11.2, which are defined as

$$h^+ = \frac{h}{U}\left(\frac{D*\Delta p}{4\rho l}\right)^{1/2} \tag{1}$$

$$s^+ = \frac{s}{U}\left(\frac{D*\Delta p}{4\rho l}\right)^{1/2} \tag{2}$$

D is the characteristic scale of the test model, which is 1/2 of the height of rectangular duct while is the diameter of circular duct.

The groove structure was stuck to the internal face of the ducts. The loss reduction effect of the grooved surface was compared with that of the smooth surface.

Results and Discussions

Rectangular duct

Fig. 6 shows a distribution of static pressure along the pipeline with smooth internal surface. Static pressure of both upper surface and side surface of the inner wall were measured.

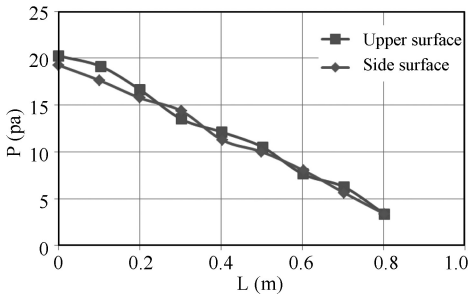

Fig. 6 Static pressure distribution of the smooth duct wall

When both the upper surface and side surface are smooth, static pressure drop along the pipeline are almost the same. It means that the experimental conditions of both sides are the same. The flow field uniformity is verified.

In order to obtain universally applicable results, data dimensionless is adopted. Loss coefficient λ is calculated to demonstrate the flow loss along the duct model at certain Reynolds numbers.

$$\lambda = \frac{\Delta p_l}{(\rho U^2/2)} \tag{3}$$

$$\Delta p_l = P_{ot} - P_{it} \tag{4}$$

$$U^2 = (P_{ot} - P_{os})/(0.5\times\rho) \tag{5}$$

The comparison of loss coefficient distribution with smooth surface and grooved surface at different Reynolds numbers is shown in Fig.7.

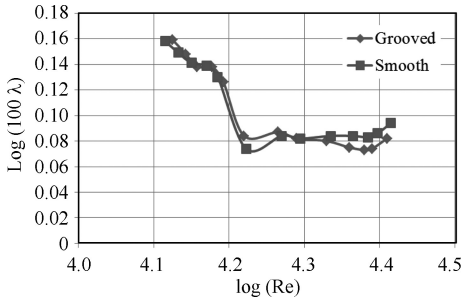

Fig. 7 Loss coefficient distribution at different Reynolds numbers

As shown in Fig.7, within the test range from1.28×10^4 to 2.57×10^4, the loss reduction of smooth surface is lower when Re is less than 1.4×10^4. When Re is between 1.4×10^4 and 1.5×10^4, the difference between loss reduction of smooth and grooved surface is tiny. When Re is between 1.5×10^4 and 1.85×10^4, the loss reduction of smooth surface is smaller. When Re increases from 1.85×10^4 to 2.0×10^4, loss reduction of smooth and grooved surface are almost the same. As Re is higher than 2.0×10^4, the effect of loss reduction is conveyed more significant. When Re is 2.4×10^4, the loss reduction efficiency reaches the maximum 2.3%−2.4%.

Circular duct

In order to apply the results of this experiment to practical world, the data dimensionless is conducted. Loss coefficient λ is calculated to demonstrate the flow loss along the duct model.

$$\lambda = \frac{\Delta p_l}{(\rho U^2/2)} \tag{6}$$

$$\Delta p_l = P_{ot} - P_{it} \tag{7}$$

$$U^2 = (P_{ot} - P_{os})/(0.5\times\rho) \tag{8}$$

$$\mathrm{Re} = \rho UD/\mu \tag{9}$$

Loss coefficients with smooth and grooved surface at three different Reynolds numbers of 7.74×10^4, 1.5×10^5 and 3.0×10^5 are calculated.

Loss coefficient distribution of the duct outlet at three Reynolds numbers with the smooth internal surface and the grooved internal surface are demonstrated in Fig.8 and Fig.9. Fig.10−12 show the different effect of smooth and grooved surface at three different Reynolds numbers respectively.

The whole loss coefficient is obtained by using area average. Fig. 13 shows the area averaged results. Under three different conditions, loss on grooved surface is

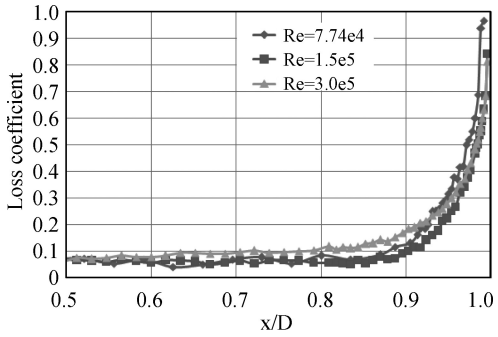

Fig. 8 Loss coefficient distribution of the duct outlet with the smooth surface

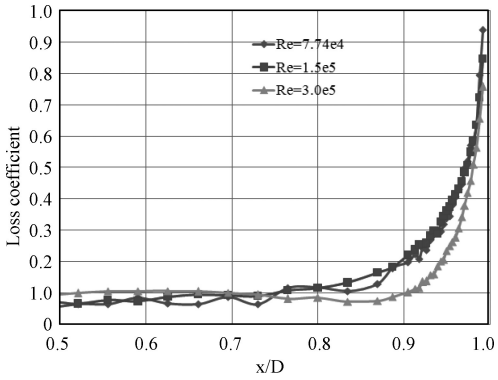

Fig. 9 Loss coefficient distribution of the duct outlet with the grooved surface

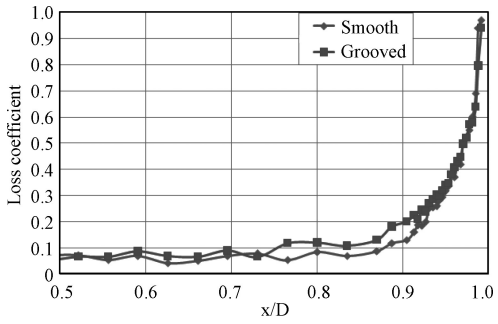

Fig. 10 Loss coefficient distribution of the duct outlet when Re is 7.74×10^4

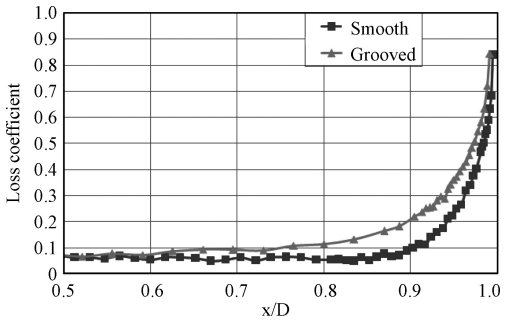

Fig. 11 Loss coefficient distribution of the duct outlet when Re is 1.5×10^5

smaller than on smooth surface. When Reynolds number of flow is 3.0×10^5, the difference between smooth and grooved surface is the most obvious among three different Reynolds numbers.

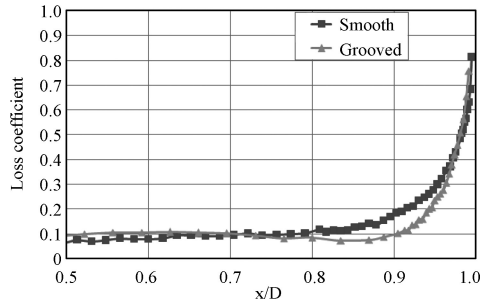

Fig. 12 Loss coefficient distribution of the duct outlet when Re is 3.0×10^5

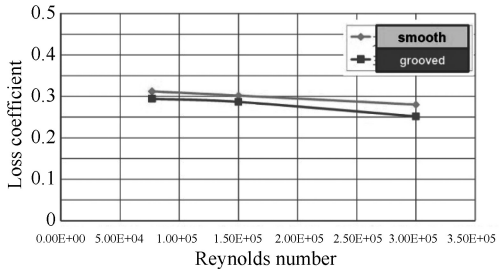

Fig. 13 Loss coefficient at three different Reynolds numbers

Loss reduction efficiency η was employed to evaluate the effect of drag reduction of the grooved surface compared with the smooth surface.

$$\eta = \left(\lambda_{smo} - \lambda_{gro}\right)/\lambda_{smo} \tag{10}$$

In Fig.14, compared with the smooth surface, the grooved surface can reduce the loss by 5.7%, 5.2% and 10% when Reynolds numbers are 7.74×10^4, 1.5×10^5 and 3.0×10^5.

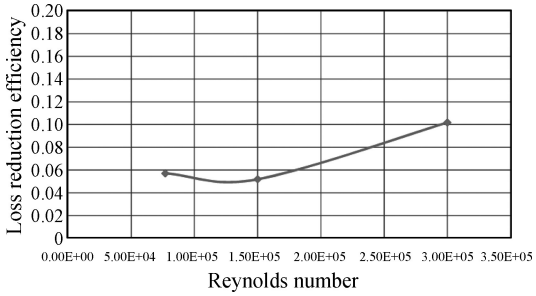

Fig. 14 Loss coefficient efficiency at three different Reynolds numbers

Conclusions

In this paper, the flow losses in rectangular and circular duct models with smooth and grooved surfaces are experimentally investigated. The effect of certain grooved structure on drag reduction is proved.

In the experiment of rectangular duct, total pressure at both inlet and outlet was measured while static pressure with smooth and grooved film was measured along the pipeline. In the experiment of the circular duct, one boundary layer pressure probe was used to measure the total pressure distribution. Static pressure was measured at inlet and outlet.

The test result indicated that this kind of grooved surface can reduce the pipe pressure loss. In rectangular duct, when Re is larger than 2.0×10^4, the effect of loss reduction becomes more significant. When Re is 2.4×10^4, the loss reduction efficiency can reach 2.3% to 2.4%. In circular duct, the loss coefficient of grooved surface is smaller than the loss coefficient of smooth surface at three tested Reynolds numbers of 7.74×10^4, 1.5×10^5 and 3.0×10^5. The loss reduction efficiency is 5.7%, 5.2% and 10% respectively. The maximum loss reduction efficiency can reach 10% at the Reynolds number of 3.0×10^5.

Acknowledgement

This work was funded by the National Natural Science Foundation of China, Grant No. 51161130525 and 51136003, supported by the 111 Project, No. B07009.

References

[1] Walsh, M.J.: Drag and heat transfer on surfaces with small longitudinal fins. AIAA Pap. No. 78−1161, (1978)

[2] Walsh, M.J.: Drag characterization of V-groove and traverse curvature riblets. In: Viscous Drag Reduction (ed. Hough, G.H.), Vol.72, Progress in Astronautics and aeronautics, pp.168−184, (1979)

[3] Walsh, M.J.: Turbulent boundary layer drag reduction using riblets. AIAA Pap. No. 82-0169, (1982)

[4] Walsh, M.J.: Riblets as a drag reduction technique. AIAA J.21. No. 4, 485−486, (1983)

[5] Walsh, M.J.: Riblets. In: Prog. Astronaut. Aeronaut. 123, 203−261, (1990)

[6] GONG Wu-Qi: Experiment study on the Mechanism of Riblets Drag Reduction, Journal of Engineering Thermophysics, Vol.23, No.5, (Sep., 2002) (in Chinese)

[7] Bushnell, D.M.: Turbulent drag reduction for external flows. Aircraft drag prediction and reduction. AGARD R-723, 5-1 to 5-26, (1985)

[8] J.J.Rohr: A comparison of the drag-reducing benefits of riblets in internal and external flows, Experiments in Fluids 13, 361−368, (1992)

[9] A.R. Moore and M.V. Lowson: Drag Reduction in a Rectangular Duct Using Riblets, Aeronautical Journal, (May., 1995)

[10] MA Hongwei, TIAN Qiao and WU Hui. Experimental Study of Turbulent Boundary Layers on Groove/Smooth Flat Surfaces. Journal of Thermal Science, 2005(3): 193−197